

1 **Highlight and Breakthrough for the paper of Liu et al. (2019) #6805**

2 **Neither antigorite nor its dehydration is “metastable”**

3 **Revision 3 (20/02/2019)**

4 Thomas P. Ferrand¹

5 1: Earthquake Research Institute, University of Tokyo, 1-1-1 Yayoi, Bunkyo-ku, Tokyo 113-0032, Japan.

6 *ferrand@eri.u-tokyo.ac.jp*

7

8 (keep metadata here for editorial office)

9 **Keywords: Antigorite, serpentine, metastability, dehydration, dehydroxylation, earthquake,**
10 **DDST, dehydration-induced seismicity, subduction.**

11

12 At confining pressures up to 6 GPa (200 km depth), antigorite is the most abundant
13 hydrous phase in the mantle between 300 and 700 °C (Wunder and Schreyer 1997). Therefore,
14 the dehydration of antigorite has been studied for decades as it is considered as the most
15 probable trigger of earthquakes in the mantle of subducting slabs (10 to 40 km below the
16 subduction interface; e.g. Peacock 2001; Hacker et al. 2003; Abers et al. 2013).

17 Liu et al. (2019) studied the kinetics of antigorite dehydration at 1 atm using non-
18 isothermal thermogravimetric analysis, which allowed determination of activation energy
19 variations as the reaction progresses (e.g. Trittschack et al. 2014; Wang et al. 2015). The results
20 show that the dehydration consists of two dehydroxylation steps (Fig. 1), as is consistent with
21 high-pressure experiments (Chollet et al. 2011). First, a slow dehydroxylation process breaks
22 low-energy OH bonds; then, high-energy OH bonds are quickly broken, leading to complete
23 antigorite breakdown. Similar experiments on chrysotile (Trittschack et al. 2014) and lizardite
24 (Zhou et al. 2017) have also indicated multi-step reaction scenarios.

25 Liu et al. (2019) confirm the fast antigorite breakdown — a key factor for seismicity.
26 Sudden stress transfers are likely to occur in the vicinity of dehydrating serpentinized faults, as
27 recently demonstrated using laboratory analogues (Ferrand et al. 2017). The latter study, along
28 with seismological observations (Cai et al., 2018; Bloch et al., 2018; Kita, and Ferrand, 2018)
29 indicate that the lower Wadati-Benioff plane of the double-seismic structure does not
30 correspond to the dehydration limit of antigorite, but rather to the hydration limit of the

31 oceanic mantle (Fig. 2). Furthermore, dehydration-induced earthquakes have been
32 demonstrated experimentally for both > 0 and < 0 volume changes, which suggests that the
33 earthquakes are triggered by dehydration itself while the resulted fluids are only a secondary
34 factor.

35 Under subduction conditions, antigorite dehydration is not “seismic” (Chernak and
36 Hirth 2010, 2011; Okazaki and Hirth 2016; Gasc et al. 2011). When a ratio of heating rate to
37 strain rate typical for real slabs (100 – 10,000 K) is applied, antigorite-olivine mixtures undergo
38 seismic events (Ferrand et al. 2017). Most likely, a dehydration-driven stress transfer triggers
39 the earthquakes in fresh peridotite at the tip of dehydrating faults (Dehydration-Driven Stress
40 Transfer model; Ferrand et al. 2017) whereas ductile deformation is dominant in serpentinites,
41 as supported by experiments (Chernak and Hirth 2011; Gasc et al. 2011) and field observations
42 (Scambelluri et al. 2017; Plümper et al. 2017).

43 Antigorite “metastability” was invoked to explain why its dehydration curve does not
44 fully fit the lower plane of the double-seismic structure (Fig. 2; e.g. Peacock 2001). Part of this
45 seismicity cannot be explained by antigorite dehydration (e.g. Abers et al. 2013), even
46 considering various compositions and environments (Ferrand 2019). However, some
47 experimental work demonstrated that, at pressures between 1 and 6 GPa (35 to 200 km),
48 antigorite dehydrates quickly in the stability field of Fo + En + H₂O (above 600 to 700 °C), which
49 suggests that subducting slabs do not contain “metastable” antigorite (Inoue et al. 2009;
50 Ferrand et al. 2017).

51 In the MgO-SiO₂-H₂O system, antigorite has 12 ideal discrete compositions depending
52 on P and T (Wunder et al. 2001), which makes it an atypical serpentine variety. Additional
53 chemical variability (e.g. the FeO-Fe₂O₃-MgO-Al₂O₃-SiO₂-H₂O system) is taken into account by
54 the general formula $M_{3m-3}T_{2m}O_{5m}(OH)_{4m-6}$ (Kunze 1961) where M and T are the octahedral
55 (Mg^{2+} , Fe^{2+} , Ni^{2+} , Al^{3+}) and tetrahedral (Si^{4+} , Al^{3+} , Fe^{3+}) cationic sites, respectively, and m is the
56 wavelength, i.e. the number of tetrahedra in a single chain along the a-axis. For natural
57 antigorite, $m = \llbracket 13; 24 \rrbracket$, which corresponds to $\approx 12.5 > C_{H_2O} > \approx 12$ wt.% (Mellini et al., 1987). In
58 other words, each polysomatic reaction (reduction of m with increasing T or decreasing P;
59 Wunder et al. 2001) is a minor dehydration reaction.

60 Antigorite stability is known to depend on H₂O saturation (e.g. Perrillat et al. 2005;
61 Hilairret et al. 2006). Perrillat et al. (2005) showed that a “talc-like” phase (5-13 wt.% H₂O)
62 forms along with olivine at H₂O-unsaturated conditions, whereas antigorite remains stable

63 under H₂O saturation. The stability limit gradually shifts toward higher temperatures with
64 increasing H₂O activity, with a maximum at the point of saturation (Perrillat et al. 2005). In
65 addition, polysomatism is expected to release up to 4% of the H₂O content of antigorite
66 (Wunder et al. 2001). The progressive H₂O loss stabilizes antigorite and is easily
67 accommodated by further hydration reactions, which enhances serpentinization between the
68 planes (Fig. 2) and forms other hydrous phases that are stable at high P-T conditions.

69 A mineral is metastable when it persists for an unbounded time outside of its stability
70 field. The kinetics of a metamorphic reaction depends on the presence of a fluid phase, which
71 promotes the mobility of atoms within a rock volume (e.g. Rubie 1990). Thus, the absence of
72 fluid favors metastability. But for dehydration reactions, this kinetic effect is in competition
73 with H₂O saturation. Indeed, H₂O stabilizes antigorite (Perrillat et al. 2005). Apparent
74 “metastability” in transforming serpentinites at subduction conditions could actually be due to
75 fluid circulations within serpentinized faults, allowing ions mobility between different regions
76 of the serpentinized zone. Fluid percolation and repeated circulation events may allow some
77 reaction products to migrate, as a supercritical fluid, up to the subduction channel. In other
78 words, the uncertainty over local variations of mantle composition and connectivity of
79 potential fluid pathways may be mistaken for “metastability”. The latter may also refer to the
80 difference in the stability limit in the P-T diagram between nominally pure phases and natural
81 minerals with variable compositions (Ferrand 2019).

82 Stability limits and dehydration processes differ between serpentine varieties (Fig. 1).
83 At atmospheric pressure, lizardite undergoes dehydroxylation between 550 and 625 °C
84 (Trittschack and Grob y 2013; Zhou et al. 2017), with a minimum activation energy of
85 $\approx 220 \text{ kJ}\cdot\text{mol}^{-1}$. Chrysotile exhibits a progressive dehydration between 500 and 650 °C, where
86 the dehydroxylation temperature depends on the nanotube diameter and is higher in the
87 innermost layers compared to the less curved outer parts of the chrysotile fibres. Its activation
88 energies range from 240 to 300 $\text{kJ}\cdot\text{mol}^{-1}$. For antigorite ($m = 17$), Liu et al. (2019) show that its
89 dehydroxylation occurs over a wide temperature range, from ≈ 450 to $\approx 775^\circ\text{C}$, followed by a
90 sharp breakdown step with a higher activation energy ($\approx 300 \text{ kJ}\cdot\text{mol}^{-1}$). At high pressures, these
91 values are expected to change, but the two-step mechanism should remain.

92 Under unsaturated conditions, talc-like phases form during the dehydration of
93 antigorite (Perrillat et al. 2005), chrysotile (Trittschack et al. 2014) and lizardite (Gualtieri et al.
94 2012). The progressive fragmentation of silicate sheets enables a transition from directional to

95 3D mobility of H₂O through the structure of dehydrated serpentine minerals. Eventually, talc-
96 like phases dehydroxylate during the last stage of chrysotile dehydration (Trittschack and
97 Grobéty 2013), similar to that observed in the high-P experiments on antigorite (Perrillat et al.
98 2005).

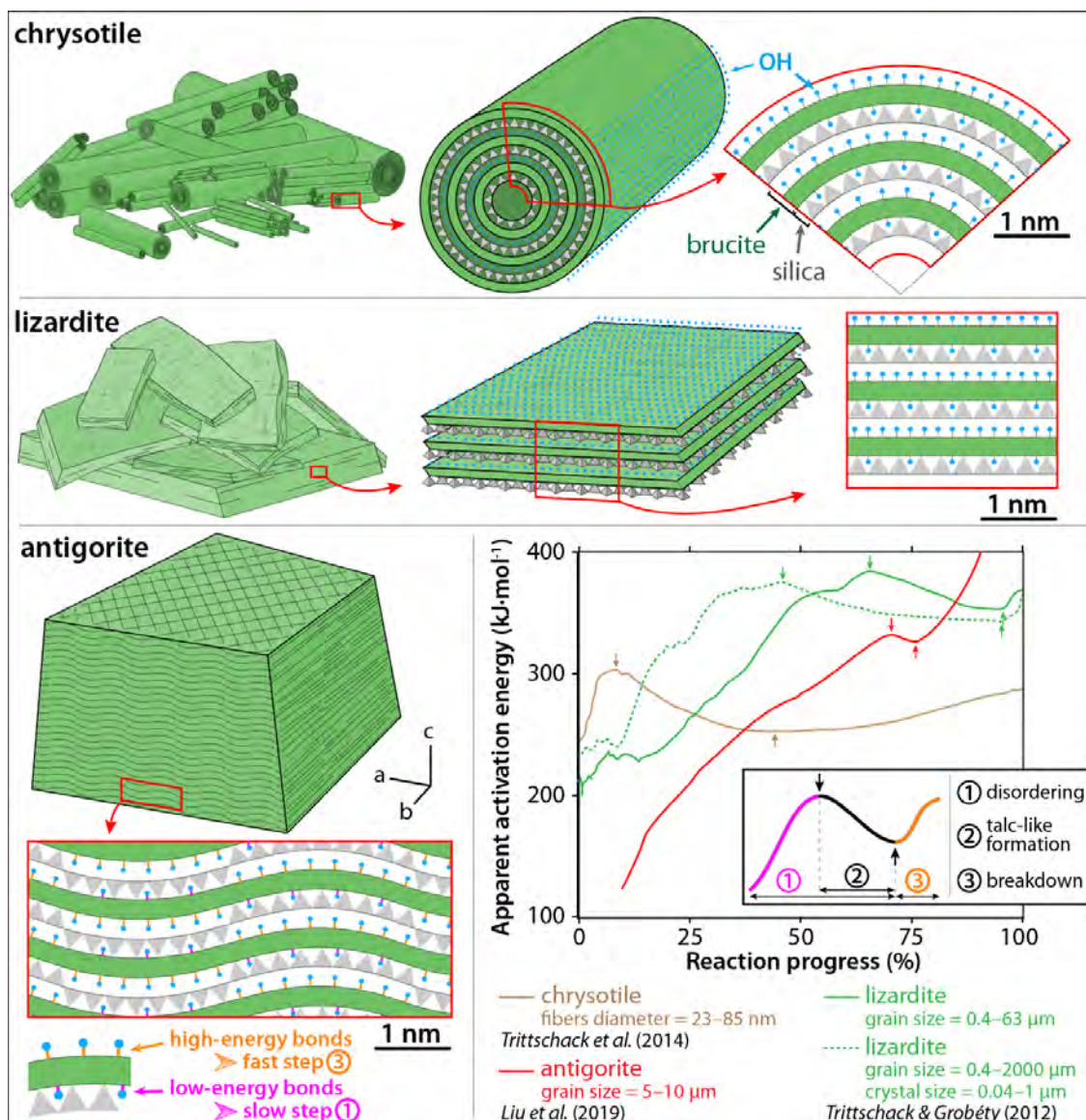
99 The structure of antigorite contains connected nanopores enabling water flow (Tutolo
100 et al. 2016; Schwarzenbach 2016), which helps deep mantle hydration near oceanic ridges (e.g.
101 Dunn et al. 2018) or at trenches (Cai et al. 2018; Shillington 2018). These pathways may also
102 facilitate H₂O redistribution within the subducting slab. Antigorite-rich rocks may, depending
103 on antigorite connectivity, drain dehydration fluids from the lower plane through the interior
104 of the double-seismic zone (Fig. 2).

105 Dehydrating antigorite forms anastomosed channels within serpentinites (Plümpert et
106 al. 2017), which consist of a mixture of olivine, talc-like and disordered serpentine. It is unclear
107 whether the permeability of dehydrating antigorite would be higher or lower than the
108 permeability of original antigorite itself. Thus, additional work is needed to understand how
109 the sudden dehydration documented by Liu et al. (2019) could trigger or inhibit further
110 dehydration.

111 Dehydration fluids transiently exist along the lower plane, as recently revealed by the
112 high V_p/V_s ratio beneath northern Chile (Bloch et al. 2018). Supercritical H₂O rapidly diffuses as
113 defects within olivine (Bai and Kohlstedt 1992), which may explain why the dehydration fluids
114 are only seen near the lower plane. The sudden dehydration would promote the production of
115 such abnormally deep fluid H₂O.

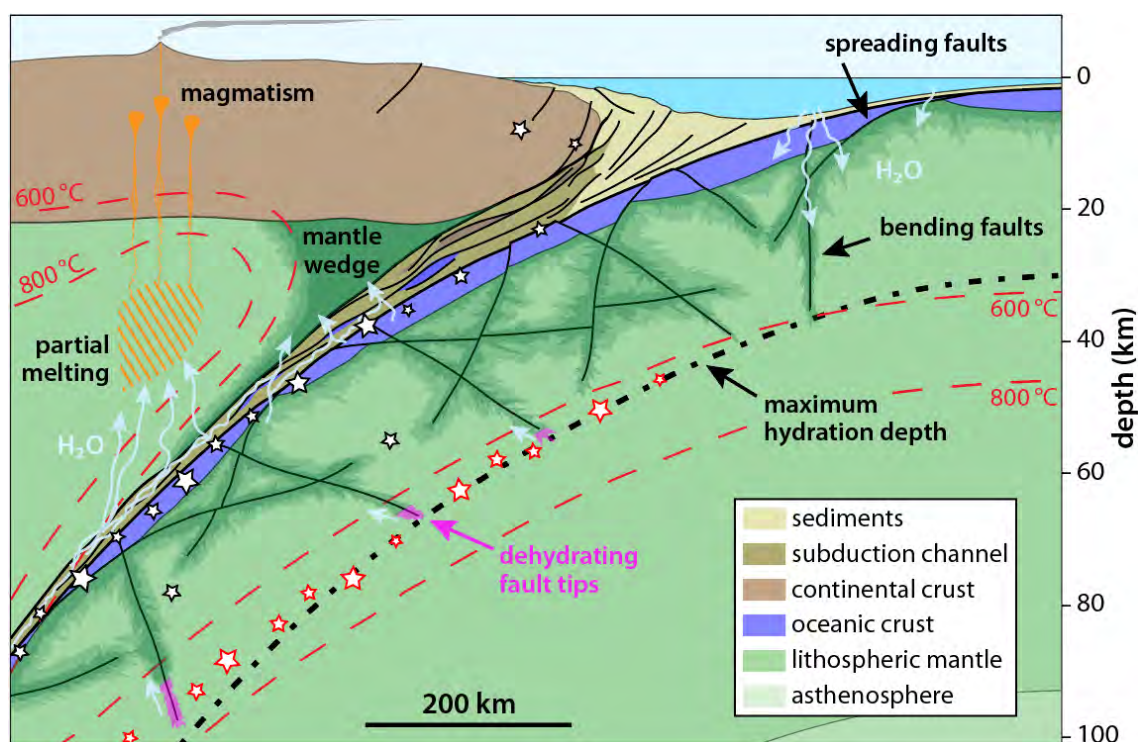
116 The study of Liu et al. (2019) confirms that antigorite dehydration is fast enough to
117 trigger brittle failure under subduction conditions (Perrillat et al. 2005; Chollet et al. 2011;
118 Ferrand et al. 2017; Inoue et al. 2009). This is also the case for other hydrous phases, e.g. talc
119 and 10-Å phase (Chollet et al. 2009). Dehydration reactions of single phases are typically fast.
120 Such transformations produce extremely fine mineral aggregates, are prone to initiate strain
121 localization by thermal runaway (e.g. Thielmann 2017), and promote critical stress transfers
122 triggering mechanical instabilities (Ferrand 2017). The stability limit of antigorite depends on
123 chemistry, fluid mobility and saturation conditions. Finally, as antigorite is not “metastable”
124 under subduction conditions, if some of the seismicity does not correlate with antigorite
125 dehydration, the decomposition of other hydrous or carbonated phases needs to be
126 considered (Ferrand 2019).

127 Through this experimental work, Liu et al. (2019) also recall the relevance of 1-atm
 128 experiments and their non-isothermal TGA provides insight as to how an antigorite crystal
 129 destabilizes, answering a question that high-pressure experiments could not fully address.



130
131
132
133

Figure 1. The dehydroxylation mechanism of serpentine minerals. Chrysotile, lizardite and antigorite have different structures, which control their stability limits and dehydration kinetics. Arrows indicate the expected limits of existence of talc-like on the activation energy curves.



134
135
136
137

Figure 2. Antigorite dehydration and double seismic zone. Stars represent earthquakes, red for the lower Wadati-Benioff plane and white for other earthquakes. Dark green corresponds to high serpentinization near faults and in the mantle wedge.

138

139 References

- 140
141
142
143
144
145
146
147
148
149
150
151
152
153
154
155
156
157
158
159
160
1. Abers, G.A., Nakajima, J., van Keken, P.E., Kita, S., and Hacker, B.R. (2013) Thermal-petrological controls on the location of earthquakes within subducting plates. *Earth and Planetary Science Letters*, 369, 178-187.
 2. Bai, Q., and Kohlstedt, D. L. (1992) Substantial hydrogen solubility in olivine and implications for water storage in the mantle. *Nature*, 357(6380), 672.
 3. Bloch, W., John, T., Kummerow, J., Salazar, P., Krüger, O. S., and Shapiro, S. A. (2018) Watching Dehydration: Seismic Indication for Transient Fluid Pathways in the Oceanic Mantle of the Subducting Nazca Slab. *Geochemistry, Geophysics, Geosystems*, 19(9), 3189-3207.
 4. Cai, C., Wiens, D.A., Shen, W., and Eimer, M. (2018) Water input into the Mariana subduction zone estimated from ocean-bottom seismic data. *Nature*, 563, 389-392.
 5. Chernak, L., and Hirth G. (2010) Deformation of antigorite serpentinite at high temperature and pressure. *Earth and Planetary Science Letters*, 296 (1-2), 23-33.
 6. Chernak, L., and Hirth G. (2011) Syndeformational antigorite dehydration produces stable fault slip. *Geology*, 39 (9), 847-850.
 7. Dunn, R.A., Arai, R., Eason, D.E., Canales, J.P., and Sohn, R.A. (2017) Three-Dimensional Seismic Structure of the Mid-Atlantic Ridge: An Investigation of Tectonic, Magmatic, and Hydrothermal Processes in the Rainbow Area. *Journal of Geophysical Research: Solid Earth*, 122, (12), 9580-9602.
 8. Ferrand, T.P., Hilairet, N., Incel, S., Deldicque, D., Labrousse, L., Gasc, J., ..., and Schubnel, A. (2017) Dehydration-driven stress transfer triggers intermediate-depth earthquakes. *Nature Communications*, 8.

- 161 9. Ferrand, T.P. (2019) Seismicity and mineral destabilizations in the subducting mantle up to 6
162 GPa, 200 km depth. *Lithos*.
- 163 10. Gasc, J., Schubnel, A., Brunet, F., Guillon, S., Mueller, H., and Lathe, C. (2011) Simultaneous
164 acoustic emissions monitoring and synchrotron X-ray diffraction at high pressure and
165 temperature: Calibration and application to serpentinite dehydration. *Physics of Earth and
166 Planetary Interiors*, 189, 121-133.
- 167 11. Gualtieri, A. F., Giacobbe, C., and Viti, C. (2012) The dehydroxylation of serpentine group
168 minerals. *American Mineralogist*, 97(4), 666-680.
- 169 12. Kita, S., and Ferrand, T.P. (2018) Physical mechanisms of oceanic mantle earthquakes:
170 Comparison of natural and experimental events. *Scientific Reports*, 8, 17049.
- 171 13. Hacker, B.R., Peacock, S.M., and Abers, G.A. (2003) Subduction factory: 2. Intermediate-depth
172 earthquakes in subducting slabs are linked to metamorphic dehydration reactions. *Journal of
173 Geophysical Research: Solid Earth*, 108.
- 174 14. Inoue, T., Yoshimi, I., Yamada, A., and Kikegawa, T. (2009) Time-resolved X-ray diffraction
175 analysis of the experimental dehydration of serpentine at high pressure. *Journal of
176 Mineralogical and Petrological Sciences*, 104(2), 105-109.
- 177 15. Liu, T., Wang, D., Shen, K., Liu, C., and Yi, L. (2019) Kinetics of antigorite dehydration, *American
178 Mineralogist*.
- 179 16. Chollet, M., Daniel, I., Koga, K. T., Petitgirard, S., and Morard, G. (2009) Dehydration kinetics of
180 talc and 10 Å phase: Consequences for subduction zone seismicity. *Earth and Planetary Science
181 Letters*, 284(1-2), 57-64.
- 182 17. Chollet, M., Daniel, I., Koga, K. T., Morard, G., and van de Moortèle, B. (2011) Kinetics and
183 mechanism of antigorite dehydration: Implications for subduction zone seismicity. *Journal of
184 Geophysical Research: Solid Earth*, 116, 1-9.
- 185 18. Kunze, G. (1961) Antigorit. Strukturtheoretische Grundlagen und ihre praktische Bedeutung für
186 die weitere Serpentin-Forschung. *Fortschritte in Mineralogie*, 9, 206-324.
- 187 19. Mellini, M., Trommsdorff, V., Compagnoni, R. (1987) Antigorite polysomatism: behaviour
188 during progressive metamorphism. *Contributions to Mineralogy and Petrology*, 97, 147-155.
- 189 20. Perrillat, J.-P., Daniel, I., Koga, K.T., Reynard, B., Cardon, H., and Crichton W. A. (2005) Kinetics
190 of antigorite dehydration; a real-time X-ray diffraction study. *Earth and Planetary Science
191 Letters*, 236, 899-913.
- 192 21. Hilairet, N., Daniel, I., and Reynard, B. (2006) Equation of state of antigorite, stability field of
193 serpentines, and seismicity in subduction zones. *Geophysical Research Letters*, 33(2).
- 194 22. Okazaki, K., and Hirth, G. 2016. Dehydration of lawsonite could directly trigger earthquakes in
195 subducting oceanic crust. *Nature*, 530(7588), 81.
- 196 23. Plümper, O., John, T., Podladchikov, Y. Y., Vrijmoed, J. C., and Scambelluri, M. (2017) Fluid
197 escape from subduction zones controlled by channel-forming reactive porosity. *Nature
198 Geoscience*, 10(2), 150.
- 199 24. Peacock, S. (2001) Are the lower planes of double seismic zones caused by serpentine
200 dehydration in subducting oceanic mantle? *Geology*, 29(4), 299-302.
- 201 25. Rubie, D. C. (1990) Role of kinetics in the formation and preservation of eclogites. *Eclogite
202 facies rocks*, 111-140.
- 203 26. Scambelluri, M., Pennacchioni, G., Gilio, M., Bestmann, M., Plümper, O., and Nestola, F. (2017)
204 Fossil intermediate-depth earthquakes in subducting slabs linked to differential stress release.
205 *Nature Geoscience*, 10, 960-96.
- 206 27. Schwarzenbach, E. M. (2016) RESEARCH FOCUS: Serpentinization and the formation of fluid
207 pathways. *Geology*, 44(2), 175-176.
- 208 28. Shillington, D. J. (2018) Water takes a deep dive into the Mariana Trench. *Nature*, 563(7731),
209 335-336.
- 210 29. Thielmann, M. (2017) Grain size assisted thermal runaway as a nucleation mechanism for
211 continental mantle earthquakes: Impact of complex rheologies. *Tectonophysics*, 746, 611-623.

- 212 30. Trittschack, R., and Grobéty, B. (2012) Dehydroxylation kinetics of lizardite. *European Journal of*
213 *Mineralogy*, 24(1), 47-57.
- 214 31. Trittschack, R., and Grobéty, B. (2013) The dehydroxylation of chrysotile: A combined in situ
215 micro-Raman and micro-FTIR study. *American mineralogist*, 98(7), 1133-1145.
- 216 32. Trittschack, R., Grobéty, B., and Brodard, P. (2014) Kinetics of the chrysotile and brucite
217 dehydroxylation reaction: a combined non-isothermal/isothermal thermogravimetric analysis
218 and high-temperature X-ray powder diffraction study. *Physics and Chemistry of Minerals*, 41(3),
219 197-214.
- 220 33. Tutolo, B.M., Mildner, D.F.R., Gagnon, C.V.L., Saar, M.O., and Seyfried, W.E. (2016) Nanoscale
221 constraints on porosity generation and fluid flow during serpentinization: *Geology*, 44, 103-106.
- 222 34. Wang, D., Yi, L., Huang, B., and Liu, C. (2015) High-temperature dehydration of talc: a kinetics
223 study using in situ X-ray powder diffraction. *Phase Transitions*, 88(6), 560-566.
- 224 35. Wunder, B., and Schreyer, W. (1997) Antigorite: High pressure stability in the system MgO-SiO₂-
225 H₂O (MSH). *Lithos*, 41, 213-227.
- 226 36. Wunder, B., Wirth, R., and Gottschalk, M. (2001) Antigorite pressure and temperature
227 dependence of polysomatism and water content. *European Journal of Mineralogy*, 13(3), 485-
228 496.
- 229 37. Zhou, S., Wei, Y., Li, B., Ma, B., Wang, C., and Wang, H. (2017). Kinetics study on the
230 dehydroxylation and phase transformation of Mg₃Si₂O₅(OH)₄. *Journal of Alloys and Compounds*,
231 713, 180-186.
232